ELSEVIER

PII: S1359-835X(97)00039-0

Composites Part A **29A** (1998) 63–70
© 1997 Elsevier Science Limited
Printed in Great Britain. All rights reserved
1359-835X/98/$19.00

Prediction of thermo-mechanical properties for compression moulded composites

G. Lielens, P. Pirotte, A. Couniot, F. Dupret and R. Keunings*
CESAME, Unité de Mécanique Appliquée, Université Catholique de Louvain, Av. G. Lemaître, 4, B-1348 Louvain-la-Neuve, Belgium
(Received 1 November 1996; accepted 13 January 1997)

We present a method to determine the thermo-mechanical properties of compression moulded composite parts. The flow-induced fibre orientation is first calculated by numerical simulation, and the resulting orientation state is used as input in a micromechanical model that predicts the thermo-mechanical properties of the part. A two-step homogenization scheme based on the grain model approach is followed. First, the properties of a reference composite with aligned fibres are estimated by means of a mixture rule between the upper and lower Hashin–Shtrikman bounds (derived by Willis). This method is in agreement with the Mori–Tanaka estimates for moderate concentrations, and gives better results for higher concentrations. Next, the properties of the composite are obtained by averaging several reference composites with different fibre directions. An example of a 3-D compression moulded composite part is analyzed and the results are discussed. © 1997 Elsevier Science Limited.

(Keywords: thermomechanical properties; compression moulding; fibre orientation; thermomechanical; micromechanics; computational modelling)

INTRODUCTION

Fibre reinforced polymers are extensively used in mass production, in view of their short shaping time in processes like injection or compression moulding, together with the good mechanical properties of the product. However, a non-homogeneous fibre orientation field is obtained which is sometimes highly anisotropic and difficult to predict for complex geometries. Thermo-mechanical properties strongly depend on fibre orientation, but also on the presence of fillers or on the part porosity. The lack of numerical tools to predict these properties can cause over-dimensioning of the parts, which results in an unwanted weight and cost increase.

The purpose of this paper is to model the whole compression moulding process, from the flow calculation to the prediction of resulting properties. We first briefly present our flow and fibre orientation model. The multi-level homogenization scheme used to predict thermo-mechanical properties is then explained. Various types of inclusions can be taken into account in this scheme, including long or short fibres, fillers or voids. Finally the example of a SMC compression moulded container is analyzed, including mechanical loading simulation.

*CESAME, Faculté des Sciences Appliquée, Université Catholique de Louvain, Bâtiment Eider, 4–6 avenue Georges Lemaître, B-1348 Louvain-la-Neuve, Belgium. Tel: +32-10-472362; Fax: +32-10-472180.

FLOW SIMULATION AND FIBRE ORIENTATION PREDICTION

As our aim is to calculate the evolution of fibre orientation during the compression moulding of thin parts, the lubrication approximation is used to calculate the flow field (which means that pressure variations across the thickness are neglected). A particular form of the Hele–Shaw model[1–7] will be established from this approximation, in accordance with the thin-cavity limit model of Barone and Caulk[8], showing that the pressure field P satisfies the following form of the mass equation:

$$\nabla\cdot(S\nabla P)+\dot{h}=0, \tag{1}$$

where S is the fluidity, which depends on the pressure gradient, the thickness of the cavity and the rheology of the suspension, and $\dot{h}$ is the time derivative of the gap width (which differentiates the equation from the one governing injection moulding). In complex parts, $\dot{h}$ depends on the mould closing speed, but also on the local mid-surface orientation.

Our rheological and fibre orientation model is derived for the isothermal flow of a concentrated and incompressible suspension of long fibres (long as compared with the gap width). The following simplifying assumptions are introduced:

- the fibres are supposed to remain parallel to the mid-surface of the cavity, leading to a two-dimensional orientation field;

- the velocity profile in the gap is assumed to be flat, thereby giving rise to a so-called plug flow;
- a thin lubricating layer, of constant thickness δ, is assumed to be present along the walls and to govern the losses of head in the cavity; the in-plane stretching viscous forces induced by fibre–flow interaction in the core are therefore neglected with respect to the effect of friction in the skin layer;
- the 2D fibre orientation field is assumed to be governed by the flow through the Advani–Tucker theory[9,7], with a high fibre aspect ratio Ar and a vanishing interaction coefficient.

This theory, which is confirmed by experimental measurements, is still under investigation[10,11] and will be discussed in a further publication.

A sketch of the simplified gap velocity profile $v(z)$ is depicted in *Figure 1*. Using the lubication approximation, the momentum equations read

$$\nabla P = \frac{\partial}{\partial z}\left(\eta \frac{\partial v}{\partial z}\right), \tag{2}$$

$$\frac{\partial P}{\partial z} = 0, \tag{3}$$

where η is the viscosity. A first integration of eqn (2) in the gap, with the condition $\partial v/\partial z(0) = 0$, provides the velocity gradient distribution:

$$\frac{\partial v}{\partial z} = \frac{z}{\eta}\nabla P. \tag{4}$$

From the assumptions of our model, the viscosity is very high in the core (where $\partial v/\partial z$ is almost vanishing). In the skin layer, the viscosity is of the form:

$$\eta = \eta_0 \dot{\gamma}^{n-1}, \tag{5}$$

where η_0 is the viscosity at zero shear rate, n is the power index ($0 < n \leq 1$) and $\dot{\gamma}$ is the shear rate,

$$\dot{\gamma}^2 = 2D : D, \tag{6}$$

which, in Hele–Shaw flows, is well approximated by the following expression:

$$\dot{\gamma}^2 = \frac{\partial v}{\partial s}\cdot\frac{\partial v}{\partial z}. \tag{7}$$

It is easy to combine eqns (4), (5) and (7) to obtain the shear rate and viscosity distributions in the skin layer. From eqn (4), the velocity gradient distribution is thus:

$$\frac{\partial v}{\partial z} = \nabla P \|\nabla P\|^{-1+1/n}\left(\frac{z}{\eta_0}\right)^{1/n}, \quad \text{if } h-\delta < z \leq h,$$
$$= 0, \qquad \text{if } 0 \leq z < h-\delta. \tag{8}$$

Hence, as the skin is very thin ($\delta/h \ll 1$), the average velocity $\bar{v}$, which is also the core velocity, is well approximated by the expression

$$\bar{v} = -\nabla P \|\nabla P\|^{-1+1/n}\left(\frac{h}{\eta_0}\right)^{1/n}\delta. \tag{9}$$

The relation between flow rate and pressure gradient can therefore be written in the form

$$h\bar{v} = -S\nabla P, \tag{10}$$

with a fluidity given by the expression

$$S = \|\nabla P\|^{-1+1/n}\frac{h^{1+1/n}\delta}{\eta_0^{1/n}}. \tag{11}$$

The mass equation is easily established from eqn (10).

According to Advani and Tucker[9], fibre orientation can be represented by using a probability distribution function $\psi(x,t,p)$, which is a function of the location x and time t, while p stands for the unit vector aligned with the fibre. Since calculating ψ means solving a four-dimensional problem in the 2D case, it is essential to simplify the model by introducing orientation tensors, which are defined as the successive moments (a_2, a_4,...) of the distribution function ψ,

$$a_2 = \oint_0 pp\,\psi(x,t,p)\,\mathrm{d}p, \tag{12}$$

$$a_4 = \oint_0 pppp\,\psi(x,t,p)\,\mathrm{d}p, \tag{13}$$

where the symbol 0 denotes the unit circle. According to the assumptions of our model, and following the Advani–Tucker theory, the evolution equation of the second order orientation tensor can be written as

$$\overset{\square}{a}_2 = -2\lambda a_4 : D_c\,, \tag{14}$$

where $\overset{\square}{a}_2$ stands for a mixed convected time derivative of a_2,

$$\overset{\square}{a}_2 = \frac{Da_2}{Dt} - \omega_c\cdot a_2 + a_2\cdot\omega_c - \lambda(D_c\cdot a_2 + a_2\cdot D_c)\,, \tag{15}$$

while Da_2/Dt is the material derivative of a_2, D_c and ω_c are the rate of strain and rotation rate tensors in the core, and λ is a function of the fibre aspect ratio,

$$\lambda = (Ar^2 - 1)/(Ar^2 + 1). \tag{16}$$

A drawback of this method is that the evolution equation for a_2 involves the fourth-order tensor a_4, which means that a closure approximation (expressing a_4 as a function of a_2) is required in order to relate the evolution of a_2 to the velocity field. We have used the natural closure approximation of Verleye and Dupret[10,12], which was shown to be more accurate than the usual quadratic or hybrid closures, especially during flow transients.

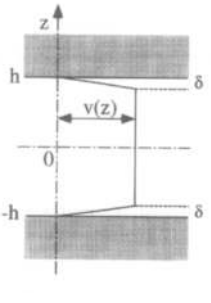

Figure 1 Simplified velocity profile in the gap

THERMO-MECHANICAL PROPERTIES

Our goal is to predict the homogenized thermo-mechanical properties everywhere in a composite part using the fibre orientation state obtained after mould filling. The composite is assumed to consist of a continuous phase (the matrix) in concentration v_m and of fibres in concentration v_i. Letting σ, ϵ, ϕ and γ denote the stress, strain, heat flux and thermal gradient, and assuming an isotropic matrix and transverse isotropic spheroidal inclusions of aspect ratio Ar, constitutive equations are written as follows:

$$- \text{ in the matrix : } \sigma = C_m : \epsilon - \beta_m \Delta T,\ \phi = k_m \cdot \tau ; \quad (17)$$

$$- \text{ in the inclusions : } \sigma = C_i : \epsilon - \beta_i \Delta T,\ \phi = k_i \cdot \tau ; \quad (18)$$

where $C_{m \text{ or } i}$, $\beta_{m \text{ or } i}$, $k_{m \text{ or } i}$ are the stiffness tensor, the thermal stress tensor and the thermal conductivity tensor of the matrix or the inclusions, respectively.

In this paper, the analysis is limited to linear materials, although the non-linear behaviour of the matrix phase is sometimes important, even if the mean stress in the composite is well below its ultimate stress. To take non linearity into account, an incremental approach using linearized constitutive equations is possible[13], with the drawback that tangent properties are not constant across the matrix phase. "Mean" tangent properties are often used to simplify the problem.

The orientation state of the inclusions is described by the second order orientation tensor a_2.

The homogenization volume is supposed to be large enough to contain a statistically representative amount of fibres, but small enough to let the orientation tensor be considered as uniform.

HOMOGENIZATION OF A TWO-PHASE COMPOSITE WITH ALIGNED INCLUSIONS

The homogenized thermo-mechanical properties of a two-phase composite depend on the properties of the inclusions and the matrix, and the distribution of strain and thermal gradient between them. This distribution can be described by introducing a fourth order deformation concentration tensor $\bar{B}^{\epsilon}$ and a second order thermal gradient concentration tensor $\bar{B}^{\gamma}$:

$$\langle \epsilon \rangle_i = \bar{B}^{\epsilon} : \langle \epsilon \rangle_m ,\ \langle \gamma \rangle_i = \bar{B}^{\gamma} . \langle \gamma \rangle_m , \quad (19)$$

where $\langle\ \rangle_{mori}$ denote the average in the matrix or the inclusions, respectively, in the homogenization volume. Using these tensors, the homogenized thermomechanical properties can be expressed as

$$\bar{C} = (v_i C_i : \bar{B}^{\epsilon} + v_m C_m) : (v_i \bar{B}^{\epsilon} + v_m I_4)^{-1} , \quad (20)$$

$$\bar{k} = (v_i k_i \cdot \bar{B}^{\gamma} + v_m k_m) \cdot (v_i \bar{B}^{\gamma} + v_m I_2)^{-1} , \quad (21)$$

$$\bar{\beta} = v_i \beta_i + v_m \beta_m + v_i v_m (C_i - C_m) : (\bar{B}^{\epsilon} - I_4) : (v_i \bar{B}^{\epsilon} + v_m I_4)^{-1} : (C_i - C_m)^{-1} : (\beta_i - \beta_m) . \quad (22)$$

Details are given in Appendix A.

Simple bounds for these tensors can be obtained without any assumption about the geometry of the phases by using the Voigt or Reuss hypotheses:

- for the Voigt bound, strain and thermal gradient are the same in the matrix and the inclusions:

$$\bar{B}^{\epsilon} = I_4 ,\ \bar{B}^{\gamma} = I_2 . \quad (23)$$

- for the Reuss bound, stress and thermal flux are the same in the matrix and the inclusions:

$$\bar{B}^{\epsilon} = C_i^{-1} : C_m ,\ \bar{B}^{\gamma} = k_i^{-1} \cdot k_m . \quad (24)$$

These bounds are too wide to be useful, but tighter bounds can be obtained for the $\bar{B}$ tensors by using geometrical information about the inclusions. The Hashin–Shtrickman–Willis bounds[14] are established for a randomly dispersed set of aligned ellipsoidal inclusions, which gives:

– as lower bounds :

$$^{lo}\bar{B}^{\epsilon} = (I_4 + E_{C_m, Ar} : (C_m^{-1} : C_i - I_4))^{-1} ,$$

$$^{lo}\bar{B}^{\gamma} = (I_2 + E_{k_m, Ar} : (k_m^{-1} \cdot k_i - I_2))^{-1} , \quad (25)$$

– as upper bounds :

$$^{up}\bar{B}^{\epsilon} = (I_4 + E_{C_i, Ar} : (C_i^{-1} : C_m - I_4)) ,$$

$$^{up}\bar{B}^{\gamma} = (I_2 + E_{k_i, Ar} : (k_i^{-1} : k_m - I_2)) , \quad (26)$$

where I_4 and I_2 are the fourth and second order unit tensors, $E_{C,Ar}$ is the fourth order Eshelby tensor[15,16] of eigenstrain concentration in a spheroidal inclusion of aspect ratio Ar if the material has a stiffness C, and $E_{k,Ar}$ is the second order Eshelby tensor[16] of eigen thermal gradient concentration in a spheroidal inclusion of aspect ratio Ar if the material has a conductivity of k.

The Mori–Tanaka theory[17], which gives exact homogenized properties for dilute concentrations (i.e. when fibres do not interact), predicts $\bar{B}$ tensors that coincide with the lower bounds of eqn (25). The upper bounds of eqn (26) can also be obtained by using the Mori–Tanaka method, by considering that fibres become the continuous phase, and that the matrix becomes the dispersed phase with an ellipsoidal geometry. The upper bounds are thus accurate estimates of the $\bar{B}$ tensors for very high concentrations (which are reached above the maximum fibre packing, when the matrix becomes dilute and discontinuous). An accurate prediction of $\bar{B}$ can therefore be obtained in the intermediate concentration range by using a mixture rule between the lower and upper bounds:

$$\bar{B}^{\epsilon} = ((1 - F_{mel}(v_i))(^{lo}\bar{B}^{\epsilon})^{-1} + F_{mel}(v_i)(^{up}\bar{B}^{\epsilon})^{-1})^{-1} ,$$

$$\bar{B}^{\gamma} = ((1 - F_{mel}(v_i))(^{lo}\bar{B}^{\gamma})^{-1} + F_{mel}(v_i)(^{up}\bar{B}^{\gamma})^{-1})^{-1} . \quad (27)$$

The mixture function $F_{mel}(v_i)$ must be monotonously increasing and must satisfy $F_{mel}(0) = 0$ and $F_{mel}(1) = 1$.

Ideally, it has to be fitted to experimental data. For example, the simple function $F_{mel}(v_i) = (v_i + v_i^2)/2$ gives very good results and has been used in the present work.

A comparison between this approach and other widely used predictive models is made in *Figure 2*. For low fibre concentration (*Figure 2a*), all models are accurate. At higher concentration, however, the Halpin–Tsai and Mori–Tanaka results underestimate the elastic stiffness. Our model and the improved Halpin–Tsai[18] equations (which increase the reinforcing factor at high volume fraction) do not show this drawback. *Figure 2b* shows predictions of the stiffness of foams. In this case, the matrix is stiffer than the inclusions (voids). The Halpin–Tsai equations (improved or not) give poor predictions. Although the Mori–Tanaka theory provides better predictions, our model behaves best, especially for high void concentration. The experimental data shown in *Figure 2* are from Termonia[19].

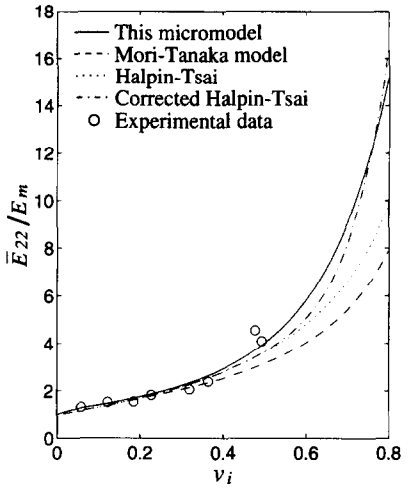

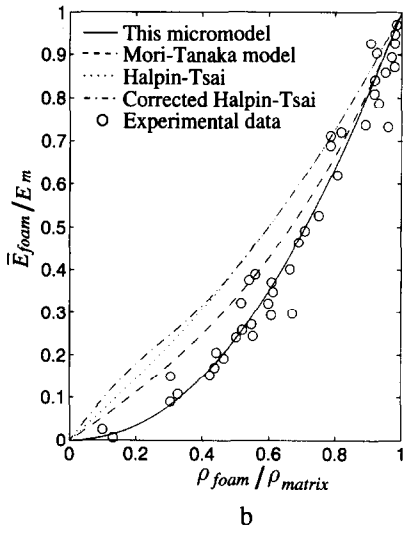

Figure 2 (a) Volume fraction dependence of the transverse Young modulus of a glass fibre/polyester composite. The fibres are aligned and continuous. (b) Density ratio dependence of the Young modulus of different foams

EXTENSION TO COMPOSITES WITH NON ALIGNED INCLUSIONS

Predicting the $\bar{B}$ tensors is difficult for a two-phase composite containing non-aligned fibres, since no precise bounds can be established as in the previous case. To tackle this problem, we have used the grain decomposition approach[20].

As represented in *Figure 3*, the representative volume is decomposed into a set of aggregates containing the matrix in the same concentration v_m as in the representative volume, and aligned fibres with a concentration $v_i = 1 - v_m$. To keep unchanged the statistical description of the representative volume (i.e. the concentration and orientation distribution of the fibres), the aggregates containing fibres of direction p must have a relative volume $dV/V_r = \psi(p)dp$. Each aggregate is first homogenized using the above described technique, in order to provide an equivalent isotropic transverse homogeneous material of stiffness $\bar{C}$, conductivity $\bar{k}$ and thermal stress $\bar{\beta}$.

In a second step, the different aggregates are themselves homogenized into a single anisotropic material, using various assumptions for the distribution of strain and thermal gradient between the aggregates. Three possible hypotheses are:

- the Voigt upper bound, which assumes a parallel assembly with constant mean strain and thermal gradient over each aggregate:

$$\bar{\bar{C}} = (\bar{C})_\psi\,,\quad \bar{\bar{k}} = \langle \bar{k} \rangle_\psi\,,\quad \bar{\bar{\beta}} = \langle \bar{\beta} \rangle_\psi\,. \tag{28}$$

- the Reuss lower bound, which assumes a series assembly with constant mean stress and thermal flux over each aggregate:

$$\bar{\bar{C}} = (\langle \bar{C}^{-1} \rangle_\psi)^{-1}\,,\quad \bar{\bar{k}} = (\langle \bar{k}^{-1} \rangle_\psi)^{-1}\,,$$

$$\bar{\bar{\beta}} = \bar{\bar{C}} : (\langle \bar{C}^{-1} : \bar{\beta} \rangle_\psi)\,. \tag{29}$$

- and the Mori–Tanaka assumption, which assumes constant mean strain and thermal gradient over the matrix of each aggregate:

$$\bar{\bar{C}} = (v_i \langle C_i : \bar{B}^\epsilon \rangle_\psi + v_m C_m) : (v_i \langle \bar{B}^\epsilon \rangle_\psi + v_m I_4)^{-1}\,,$$

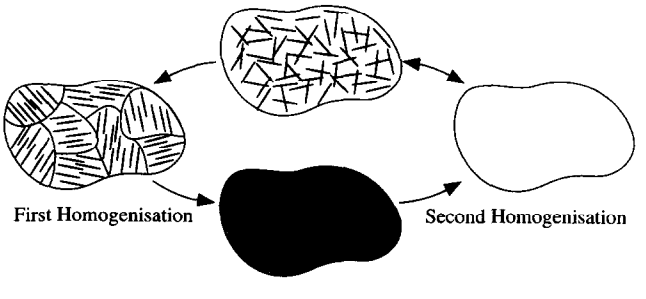

Figure 3 Grain model as a two-step homogenization method

$$\bar{\bar{k}} = (v_i\langle k_i : \bar{B}^{\gamma}\rangle_{\psi} + v_m k_m) : (v_i\langle \bar{B}^{\gamma}\rangle_{\psi} + v_m I_2)^{-1},$$

$$\bar{\bar{\beta}} = \langle v_m\beta_m + v_i(\beta_i - C_i : (I_4 - \bar{B}^{\epsilon}) : (C_i - C_m)^{-1} :$$

$$(\beta_i - \beta_m))\rangle_{\psi} + \bar{\bar{C}} : \langle v_i(I_4 - \bar{B}^{\epsilon}) : (C_i - C_m)^{-1} :$$

$$(\beta_i - \beta_m)\rangle_{\psi} . \qquad (30)$$

where $\bar{B}^{\epsilon}$ and $\bar{B}^{\gamma}$ are the concentration tensors for one aggregate with aligned inclusions.

Orientation averaging over the aggregates can be calculated directly using the a_2 and a_4 orientation tensors[9,20,21]. When a_2 is the only known orientation tensor, a_4 can be determined using the natural closure approximation.

Let us emphasize that, for two-phase composites containing inclusions of different shapes or orientations, the Mori–Tanaka assumption gives a higher estimate of stiffness or conductivity than the Voigt upper bound when the inclusions are stiffer or more conductive than the matrix, and that an estimate below the Reuss lower bound is provided in the opposite case. This can be explained as follows: consider, for instance, the stiffness of a composite containing stiffer inclusions than its matrix. The most rigid aggregates are the ones which have the highest $\bar{B}^{\epsilon}$ tensor. If the mean strain is the same in the matrix of each aggregate, the total mean strain is higher in the aggregates having a larger $\bar{B}^{\epsilon}$ tensor. The Mori–Tanaka assumption thus leads to a non-physical behaviour, the stiffest grains undergoing the largest deformation. In this work, we have therefore chosen to use the Voigt upper bound for the second homogenization. An example of aggregate averaging is given in *Figure 4*.

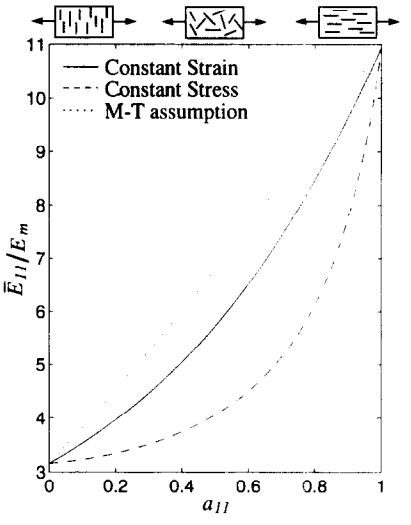

Figure 4 Longitudinal Yound modulus of a glass fibre ($Ar = 100$, $v_i = 50\%$)/polyamide 6-6 composite for different states of planar orientation

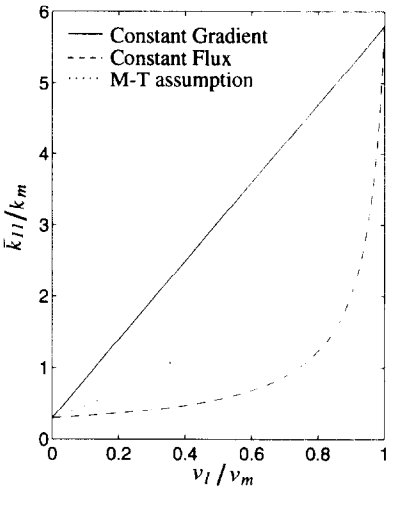

Figure 5 Thermal conductivity of a three phase composite made of perfectly conductive spheres of concentration v_1, non-conductive spheres of concentration v_2 and matrix of concentration $v_m = 50\%$

EXTENSION TO MULTIPHASE COMPOSITES

Although it is not possible to fully describe the thermo-mechanical behaviour of a multiphase composite by means of the two tensors $\bar{B}^{\epsilon}$ and $\bar{B}^{\gamma}$, it is easy to extend the grain model to composites containing more than one type of inclusion: in that case, the representative volume is decomposed into aggregates containing a matrix of concentation v_m and aligned inclusions of only one type of concentration $1 - v_m$. This set of aggregates is then homogenized using the same assumptions as previously. An example showing the prediction of conductivity for a three phase composite is given in *Figure 5*.

EXAMPLE AND DISCUSSION

We consider the filling of a 5 mm thick container with Sheet Moulding Compound (SMC). In view of symmetry, only a quarter of the part is analyzed. Data from a common polyester–glass fibre SMC have been used in isothermal flow calculations. The aspect ratio of the fibres is 1000. The fixed finite element mesh covering the whole part is represented in *Figure 6a*, while an example of temporary mesh generated during filling is shown in *Figure 6c*. The rectangular-shaped initial load and the successive fronts of material during compression are represented in *Figure 6b*. The orientation field is represented at different stages of the filling in *Figures 6d*, *e* and *f* by means of the two eigenvector–eigenvalue products of the second order orientation tensor. It is interesting to note that the final orientation state obtained by compression moulding greatly differs from what can be observed for injection moulded parts. The injection gate is indeed often followed by a divergent region, where fibres orient perpendicularly to the velocity. The final orientation is therefore rather anisotropic in injection moulding. However, in compression moulding, fibres tend to be less oriented (since a compressed isotropic disc remains isotropic, for instance). For multi-faceted parts like the container, important differences in gap width

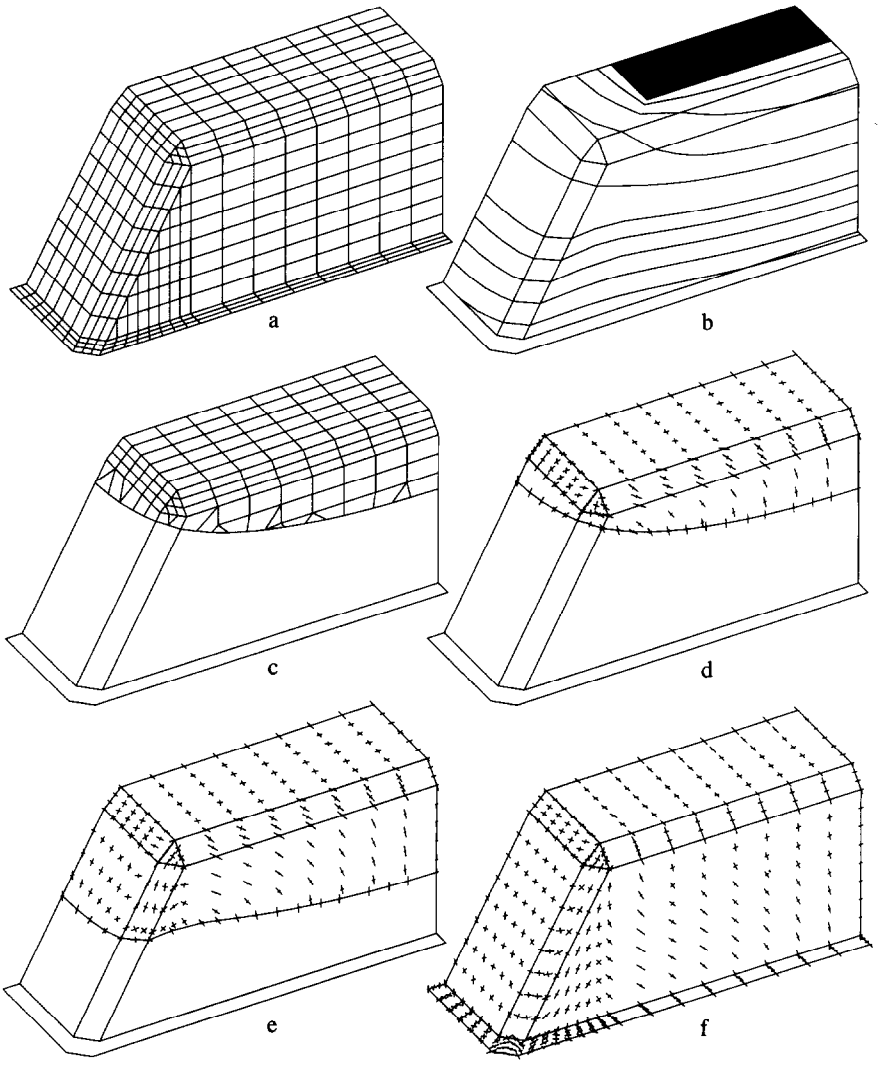

Figure 6 Compression moulding of a container: (a) fixed mesh; (b) initial load and successive flow-front; (c) temporary mesh example; (d and e) transient orientation fields during filling; (f) final orientation field. Only a quarter of the part is represented

between the facets are observed during the flow, which induce a sharp contraction tending to align the fibres with the fluid velocity (*Figures 6d* and *e*). The more compression progresses, the less this effect is important as the gap width becomes uniform at the end of the filling (*Figure 6f*). These effects, combined with in-plane deformation and transport, give rise to an unexpected final orientation pattern.

The calculated fibre orientation field in the part has been used as input to predict its thermo-mechanical properties. The bending and tension stiffness matrices have subsequently been computed for each element of the fixed mesh, using the classical Kirchoff theory, and have been introduced as a material property in the Finite Element structure computation code SAMCEF (which is able to deal with anisotropic materials). *Figure 7* shows the deformation and the von Mises stress in the container when it is clamped on its lower horizontal face and is loaded with an internal pressure of 1 bar. The behaviour of the part (*Figure 7a*) is compared to a simplified case where fibre orientation is supposed to be isotropic (*Figure 7b*). One can observe that the shape of the deformed part and the stress distribution are mainly dependent on the geometry of the part. However, the camber is significantly lower in the case of the flow-induced fibre orientation.

CONCLUSIONS

We have presented a global model that is able to predict the linear thermo-mechanical properties of complex composite parts from the flow-induced fibre orientation state. A decoupled approach has been used to calculate the flow kinematics and the fibre orientation during the compression moulding process. This model leads to qualitatively good results in the case of concentrated long fibres. The influence of fibre–fibre and fibre–polymer interactions on the flow however is neglected. Our micromechanical model is also appropriate when various types and concentrations of reinforcements are present in the composite. This model can provide a very efficient

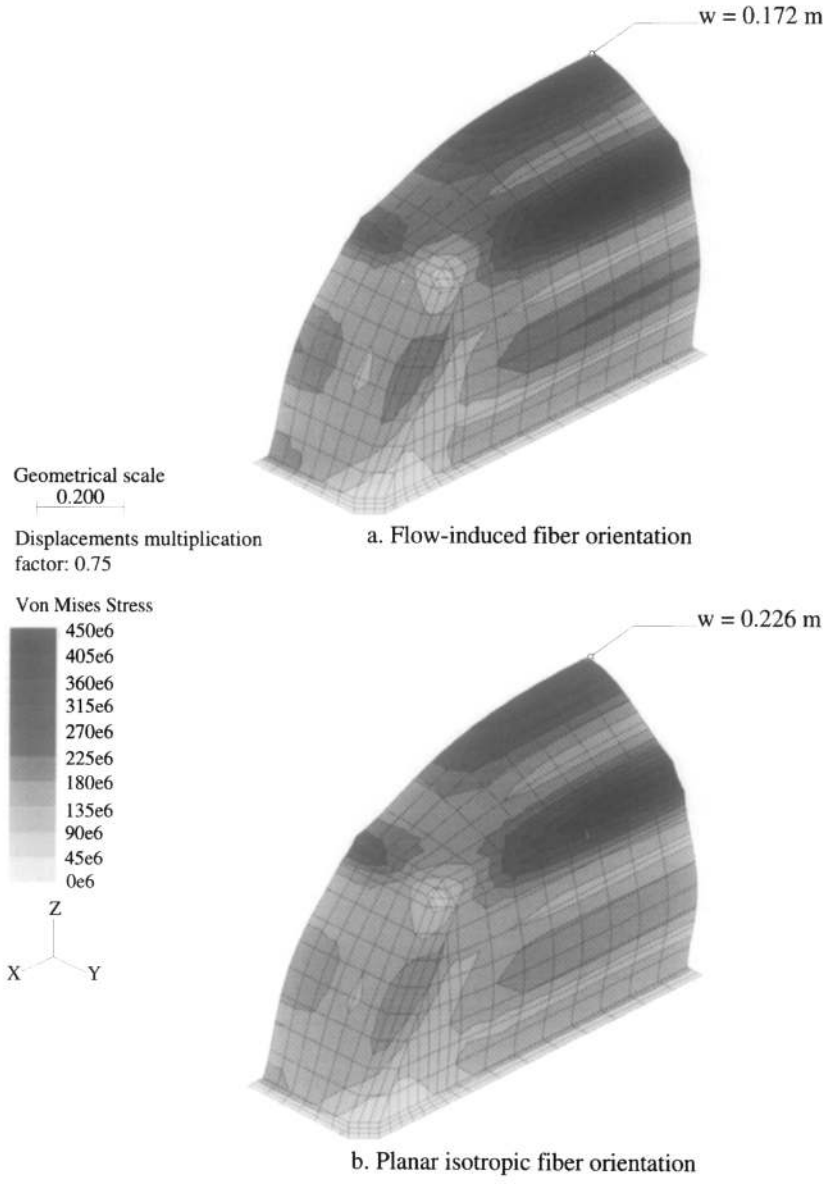

Figure 7 Behaviour of the container under 1 bar pressure. Comparison between the moulded container with the flow induced orientation and a reference case with planar isotropic orientation. Isovalues indicate the von Mises stress, and w is the camber

tool to optimize the design of composite parts, taking processing conditions into account. To validate this approach, comparisons with experimental results will be made to test both fibre orientation and thermo-mechanical properties.

ACKNOWLEDGEMENTS

The work of G. Lielens and P. Pirotte has been supported by the COST 512 European Project, locally financed by the Government of the Walloon Region, Belgium. The paper presents research results of the Belgian Program on Interuniversity Poles of Attraction, initiated by the Belgian State, Prime Minister's Office for Science, Technology and Culture. The scientific responsibility rests with its authors.

APPENDIX

The homogenised properties of a representative volume of composite are defined for imposed mean strain $<\epsilon>$, temperature ΔT and mean thermal gradient $<\gamma>$ by the following relations:

– stiffness $\bar{C}$ and thermal stress $\bar{\beta} : \langle\sigma\rangle = \bar{C} : \langle\epsilon\rangle - \bar{\beta}\Delta T$. (A1)

– thermal conductivity $\bar{k} : <\phi> = \bar{k} \cdot <\gamma>$. (A2)

To derive the expression of $\bar{C}$, a mean strain $\bar{\epsilon}$ is supposed to be imposed on a representative volume of composite. This mean strain can be expressed as a function of the mean strain in the matrix phase using the definition (19):

$$\langle\epsilon\rangle = v_i\langle\epsilon\rangle_i + v_m\langle\epsilon\rangle_m = (v_i\bar{B}^{\epsilon} + v_m I_4) : \langle\epsilon\rangle_m \qquad \text{(A3)}$$

The mean stress is obtained using the constitutive equations

(17) and (18) with $\Delta T = 0$:

$$\langle\sigma\rangle = v_i\langle\sigma\rangle_i + v_m\langle\sigma\rangle_m = v_i C_i : \langle\epsilon\rangle_i + v_m C_m : \langle\epsilon\rangle_m$$
$$= (v_i C_i : \bar{B}^{\epsilon} + v_m C_m) : \langle\epsilon\rangle_m. \quad \text{(A4)}$$

By inverting relation (A3), the mean stress can be expressed as a function of mean strain in the representative volume of composite, giving the expression (20) for $\bar{C}$. The expression (21) for $\bar{k}$ is obtained in exactly the same way.

Computing $\bar{\beta}$ is less immediate. The representative volume is supposed to undergo a temperature difference ΔT and a constant strain ϵ is imposed in all this volume. The stress must be equal in the inclusions and the matrix for equilibrium:

$$\sigma_i = C_i : \epsilon - \beta_i \Delta T = \sigma_m = C_m : \epsilon - \beta_m \Delta T$$
$$\Rightarrow \epsilon = (C_i - C_m)^{-1} : (\beta_i - \beta_m)\Delta T . \quad \text{(A5)}$$

Next, an opposte mean strain $-\epsilon$ is superposed, in such a way that the total mean strain vanishes. Using the relation (A3) and (19), the mean strain in the matrix and the inclusions can easily be computed:

$$\langle\epsilon\rangle_i = \epsilon - \bar{B}^{\epsilon} : (v_i \bar{B}^{\epsilon} + v_m I_4)^{-1} : \epsilon , \quad \text{(A6)}$$

$$\langle\epsilon\rangle_m = \epsilon - (v_i \bar{B}^{\epsilon} + v_m I_4)^{-1} : \epsilon. \quad \text{(A7)}$$

It is easy to verify that $v_i\langle\epsilon\rangle_i + v_m\langle\epsilon\rangle_m = 0$. With the help of the constitutive equations (17) and (18), the mean stress in the matrix and the inclusions is:

$$\langle\sigma\rangle_i = C_i : (I_4 - \bar{B}^{\epsilon} : (v_i \bar{B}^{\epsilon} + v_m I_4)^{-1}) : \epsilon - \beta_i \Delta T , \quad \text{(A8)}$$

$$\langle\sigma\rangle_m = C_m : (I_4 - (v_i \bar{B}_i^{\epsilon} + v_m I_4)^{-1}) : \epsilon - \beta_m \Delta T. \quad \text{(A9)}$$

Finally, the expression (22) for the homogenized thermal stress tensor $\bar{\beta}$ is obtained using the definition (A1).

REFERENCES

1. Berger, J. L. and Gogos, C. G., A numerical simulation of the cavity filling process with PVC in injection molding. *Polym. Eng. Sci.*, 1973, **13**, 102–112.
2. Lord, H. A. and Williams, G., Mold-filling studies for the injection molding of thermoplastic materials. Part II: the transient flow of plastic materials in the cavities of injection-molding dies. *Polym. Eng. Sci.*, 1975, **15**, 569–582.
3. Hieber, C. A. and Shen, S. F., A finite-element/finite-difference simulation of the injection-molding filling process. *J. Non-Newtonian Fluid Mech.*, 1980, **7**, 1–32.
4. Isayev, A. I. (Ed.), *Injection and Compression Molding Fundamentals*. Marcel Dekker, New York, 1987.
5. Dupret, F. and Vanderschuren, L., Calculation of the temperature field in injection moulding. *AIChE Journal*, 1988, **34**, 1959–1972.
6. Couniot, A., Dheur, L. and Dupret, F., Numerical simulation of injection moulding: non-isothermal filling of complex thin shapes including abrupt changes of thickness or bifurcations of the midsurface. In *Mathematical Modeling for Materials Processing, IMA New Series Number 42*, M. Cross, J.F.T. Pittman and R.D. Wood (Eds.). Clarendon Press, Oxford, 1993, pp. 381–398.
7. Crochet, M. J., Dupret, F. and Verleye, V., Injection moulding. In *Flow and Rheology in Polymer Composites Manufacturing*, S. Advani (Ed.). Elsevier, 1994, pp. 415–463.
8. Barone, M. R. and Caulk, D. A., A model for the flow of a chopped fiber reinforced polymer compound in compression molding. *J. Appl. Mech.*, 1986, **53**, 361–371.
9. Advani, S. G. and Tucker, C. L., The use of tensors to describe and predict fibre orientation in short fibre composites. *J. Rheology*, 1987, **31**, 751–784.
10. Verleye, V. and Dupret, F., Prediction of fibre orientation in complex injection moulded parts. In *Proc. of the 1993 ASME Winter Annual Meeting*, D. A. Siginer, W. E. Van Arsdale, C. E. Altan and A. N. Alexandrou (Eds.), AMD-Vol. 175, pp. 139–163.
11. Dewez, L., Pirotte, P., Lielens, G., Couniot, A. and Dupret, F., Effect of in-plane and shear viscosity on the flow and fiber orientation of long fiber injection moulded composites. In *Proc. of the FPCM'96 Conference*, J. A. Goshawk and R. S. Jones (Eds.), 1996, Session 2.
12. Verleye, V., Couniot, A. and Dupret, F., Numerical prediction of the orientation field in complex composite injection moulded parts. In *Proc. of the 1994 ASME Winter Annual Meeting*, K. Himasekhar, V., Prasad, T. A. Osswald and G. Batch (Eds.), MD-Vol 49, HTD-Vol 283, 1994, pp. 265–279.
13. Lin, S. C., Hirose, Y. and Mura, T., Constitutive equations of power-law composites and failure of materials having multiple cracks. *J. Eng. Materials and Technology*, 1994, **116**, 359–366.
14. Willis, J. R., Bounds and self-consistent estimates for the overall moduli of anisotropic composites. *J. Mech. Phys. Solids*, 1977, **28**, 185–202.
15. Eshelby, J. D., The determination of the elastic field of an ellipsoidal inclusion and related problems. *Proc. Roy. Soc. London, Ser. A*, 1957, **241**, 376–396.
16. Clyne, T. W. and Withers, P. J., An introduction to metal matrix composites. In *Cambridge Solid State Science Series*, E. A. Davis and I. M. Ward (Eds.), 1993, pp. 481–482.
17. Benveniste, Y., A new approach to the application of Mori–Tanaka's theory in composite materials. *Mechanics of Materials*, 1987, **6**, 147–157.
18. Halpin, J. C. and Kardos, J. L., The Halpin–Tsai equations: a review. *Polym. Eng. Sci.*, 1976, **16**, 344–352.
19. Termonia, Y., Computer model for the elastic properties of short fibre and particulate polymers. *J. Materials Science*, 1987, **22**, 1733–1736.
20. Camacho, C. W., Tucker, C. L., Yalvac, S. and McGee, R. L., Stiffness and thermal expansion predictions for hybrid short fibres composites. *Polym. Comp.*, 1990, **11**, 229–239.
21. Verleye, V., Lielens, G., Pirotte, P., Dupret, F. and Keunings, R., Prediction of flow-induced orientation field and mechanical properties of injection moulded parts. In *Proc. NUMIFORM 95*, S. H. Shen and P. Dawson (Eds.). Balkema, Rotterdam, 1995, pp. 1213–1218.

NOMENCLATURE

P	pressure (Pa)
$\dot{\gamma}$	strain rate (s^{-1})
h	normal closure velocity (ms^{-1})
S	fluidity of the fibre suspension in the mould ($m^3s^{-1}Pa^{-1}$)
D	strain rate tensor (s^{-1})
ω	rotation rate tensor (s^{-1})
I_2	second order unit tensor
I_4	fourth order unit tensor
p	fibre orientation unit vector
$\psi(p)$	fibre orientation distribution function
a_2	= second order orientation tensor
a_4	= fourth order orientation tensor
λ	= dimensionless parameter related to fibre aspect ratio
$\overset{\square}{a}_2$	= mixed convected derivative of a_2
σ	stress tensor (Pa)
ϵ	deformation tensor
ΔT	temperature difference (K)
ϕ	heat flux (Wm^{-2})
γ	thermal gradient (Km^{-1})
C	stiffness tensor (Pa)
β	thermal stress tensor (PaK^{-1})
k	thermal conductivity tensor ($WK^{-1}m^{-1}$)
$E_{C,Ar}$	fourth order Eshelby tensor for eigenstrain concentration for a material of stiffness C, in an spheroidal inclusion of aspect ratio Ar
$E_{k,Ar}$	second order Eshelby tensor for eigen thermal gradient concentration for a material of conductivity k, in a spheroidal inclusion of aspect ratio Ar
$< X >$	the average of the tensor X on the representative volume
$< X >_y$	the average of the tensor X on the matrix of the representative volume if $y = m$, on the inclusions of the representative volume if $y = i$
$< X >_{\psi}$	$\oint X(p)\psi(p)\mathrm{d}p$, which means average of the transverse isotropic tensor X over all the orientations